Materials Science and Engineering, A161 (1993) 75–82

The modelling of the mechanical alloying process in a planetary ball mill: comparison between theory and *in-situ* observations

P. Le Brun*, L. Froyen and L. Delaey

Department of Metallurgy and Materials Engineering, Katholieke Universiteit Leuven, De Croylaan 2, B-3001 Leuven (Belgium)

(Received March 30, 1992; in revised form September 21, 1992)

Abstract

In order to understand the mechanical alloying (MA) process in a planetary ball mill (PBM), the kinetics of a ball during milling have been analysed and the calculated ball trajectory is compared with *in-situ* observations of ball movement. Three different milling modes are deduced from the modelling. Although an experimentally efficient milling mode can be explained from the modelling, there is no good agreement between theory and *in-situ* observations in the mode of operation of most commercially available PBMs. The present study shows that, in these mills, the MA process should be described in terms of attrition and wear and not in terms of impact as is usually done.

1. Introduction

Used first in the early 1970s for the production of oxide-dispersion-strengthened (ODS) superalloys, mechanical alloying (MA) is now recognized as a versatile technique for the production of a broad range of powders, from amorphous [1] or nanocrystalline [2] to ODS [3] or intermetallics [4] among others. A complete review of the MA process has recently been published [5].

Despite the large numbers of systems already investigated, there is still only a partial understanding of the phenomena occurring during the MA process. Finding the optimal conditions for MA of a new alloy composition still relies mainly on an experimental approach.

If MA has to be fully understood, the following topics should be treated: (1) The nature and quantification of the interactions between the milling ball and the powder during MA, including a complete description of the ball kinetics during milling; (2) deformation phenomena occurring in one powder particle interacting with a milling ball (fracture, welding, oxidation, etc.); (3) physical phenomena occurring inside the powders (diffusion, heating, work hardening, oxidation, recovery, etc.). Several of these aspects have been partly treated in literature (see for example refs. 5 and 6). Planetary ball mills (PBMs) are often used for MA since they allow the study of several different blends of powders at the same time. When milling parameters are defined, sufficient quantities can be produced for consolidation and further mechanical or physical tests. The present article contributes to the analysis of the interactions between milling balls and powders in a planetary ball mill, complementing the results of a EURAM project [7]. Two approaches are usually considered to provide an understanding of the MA process in PBMs. In the first, milling parameters are related to experimental results, leading to guidelines for optimum processing. The influence of milling intensity on powders has been earlier demonstrated [8] and a more systematic approach has resulted in the construction of the so-called "parameter phase diagram" (PPD) [9], presenting the phases forming upon MA in a given material system as a function of the milling parameters. The second approach relates a modelling of the mill to experimental results [10] and aims at quantifying the MA parameters as a basis for a rational approach of the process.

In order to correlate theory and experiments, starting powders with specific and well-defined characteristics are required; they should be large enough to allow microhardness measurements, spherical in order to make visual observation of deformation possible, and ductile and easily deformable to detect even low interaction levels. Pure Cu powders have been selected. No other element was added to the Cu powders as the principal aim of the work is to study powder–ball interactions.

*Present address: Pechiny CRV, Parc Economique Centr'alp, BP 27, F-38340 Voreppe, France.

0921-5093/93/$6.00

2. Theoretical approach

In this section, trajectories of balls in the mill are calculated in order to predict the operative modes of a PBM. A PBM (Fig. 1) consists of a sun disc (rotating at a speed $\Omega = d\theta/dt$) on which milling containers are rotating in an opposite direction towards the sun disc (at a speed $\omega = d\varphi/dt$). The angular velocity ratio $R = \omega/\Omega$ is useful in the description of the kinetics of the mill. All the symbols used are listed in Appendix A.

The forces exerted on a ball in the milling container are the centrifugal forces towards the centre of the sun disc and the centre of the milling container, the friction resulting from the interactions between the ball and the milling container, and gravity. The ball is considered as a point mass represented by the movement of its centre of gravity. For this reason, friction between the ball and the milling container is not treated in this approach. For ease of analysis, the gravity force is neglected. This hypothesis is valid in the first approximation since gravity represents only a small percentage of the acceleration of the mill as operated for MA. In another modelling of PBMs, similar hypotheses were made [10]. The problem simplifies to the analysis of the movement of one single ball in a planar section. As long as the force on a ball is oriented towards the exterior of the mill, the ball is in contact with the surface of the milling container. The ball behaves as if it were attached to the container and rotates with it until an angular position where the resultant of the forces is oriented towards the centre of the mill. Once the ball leaves the surface of the milling container, the kinetics of rigid bodies are used to describe its free motion until it comes into contact again with the mill. The calculations are done on the assumption that a single ball is present in the mill.

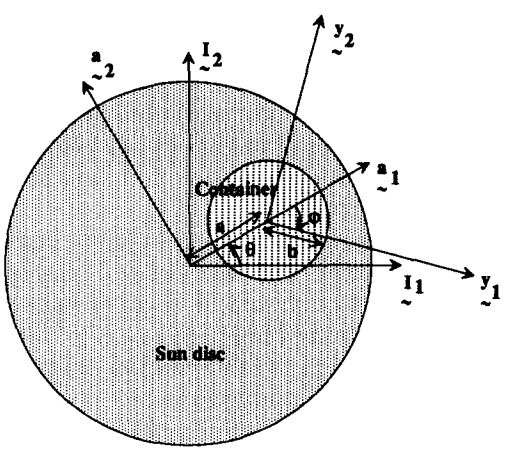

Fig. 1. Geometrical parameters of a PBM. Coordinate systems are indicated.

Using the above assumptions, the position of a ball inside the milling container can be described parametrically by (see Appendix B)

$$x_1 = t(v_1 \cos\theta + v_2 \sin\theta) + p_1 \cos\theta + p_2 \sin\theta - a \quad (1a)$$

$$x_2 = t(v_2 \cos\theta - v_1 \sin\theta) - p_1 \sin\theta + p_2 \cos\theta \quad (1b)$$

where x_1 and x_2 are expressed in the $\boldsymbol{a}_\alpha$ coordinate system. Relations written in this axis system allow visualization of the movement of the ball relative to the milling container. The initial position (p_1, p_2) and velocity $(v_1; v_2)$ are determined at the angular position on the milling container where the ball is detached. This angle φ_0 can be determined analytically (Appendix C):

$$\varphi_0 = \arccos\left(-\frac{b}{a}(1-R)^2\right) \quad (2)$$

The values φ_0 and $2\pi - \varphi_0$ define a domain on the surface of the milling container where the resultant of the forces on a ball is oriented towards the centre of the mill. Hence, a ball will never be in the stable condition on the surface of the mill between these angles φ_0 and $2\pi - \varphi_0$.

With these assumptions, the trajectory of a ball inside a milling container can be fully described. Once the ball has left the surface at the angle φ_0, its movement is described by (1a) and (1b) until it contacts the surface again $(x_1^2 + x_2^2 > b^2)$ at an angle φ_{impact}. The ball then remains in contact with the surface of the mill and rotates with it until the angle φ_0 is reached again.

Based on the calculation of the movement of a ball, three different types of trajectory are possible. These three different milling modes appear when the ratio of the milling velocities is modified. In other words, for one given mill, the trajectory of a ball depends upon the ratio of velocities and the actual milling velocity Ω has no influence on the trajectory. As will be explained below, these three modes are termed "chaotic" for $R < R_{\text{limit}}$, "impact + friction" for $R_{\text{limit}} < R < R_{\text{critical}}$ and "friction" for $R > R_{\text{limit}}$. An example of the movement of the centre of mass of a ball in the three milling modes is given in Fig. 2.

(1) *"Chaotic mode" ($R < R_{\text{limit}}$).* When the trajectory is calculated as explained, the value of the impact angle is between φ_0 and $2\pi - \varphi_0$. This means that the ball will impact on the surface and directly leave it because the force on the ball is oriented towards the interior of the mill. The movement of the ball can hardly be calculated with this model.

(2) *"Impact + friction mode ($R = R_{\text{limit}}$ to R_{critical}).* Between these two values of the ratio, the trajectory of a ball can be computed with the model developed. Further calculations can be done and involve the

energy at the time of impact which can be decomposed into two components: the first is normal to the mill surface (called the "impact component") and the second is tangential to the mill surface (called the "friction component"). They have been calculated for a specific mill, and the evolution of the two components is presented as a function of the milling ratio R in Fig. 3. The graph suggests that a mill could be designed for specific purposes depending upon the value of R. For the mill concerned in the calculations, pure impact is obtained for $R = 2.25$, whereas high friction results from values close to $R_{critical}$. Typical values of energy range from 1 to 100 mJ depending upon the parameters of the experiments.

(3) *"Friction mode" ($R > R_{critical}$).* The forces exerted on a ball are such that their resultant is never oriented towards the interior of the mill. The model foresees that the ball will always stick to the surface of the mill. The interactions between the ball and the powder can only occur during friction between the ball and the milling container and cannot be described by the model.

These operative modes of a PBM can be conveniently presented in a graph setting the angular position on the surface of the milling container (the angle φ) as a function of the ratio R (Fig. 4). For every value of R (given by a vertical line in the graph), the value of the angles φ_0 and $2\pi - \varphi_0$ are given, and the domain between them is shaded, reminding us that it is a domain where a ball cannot come into contact with the surface of the mill without leaving it directly. The value of the calculated impact angle φ_{impact} is also indicated. One cycle of movement of the ball is read in the graph as follows. For one value of R, the ball will move on a vertical line in the graph (the ball is located on the surface of the mill and is turning with it) until it crosses the curve φ_0 where it starts to fly into the milling container. When the angle φ_{impact} is reached, the ball contacts the surface again.

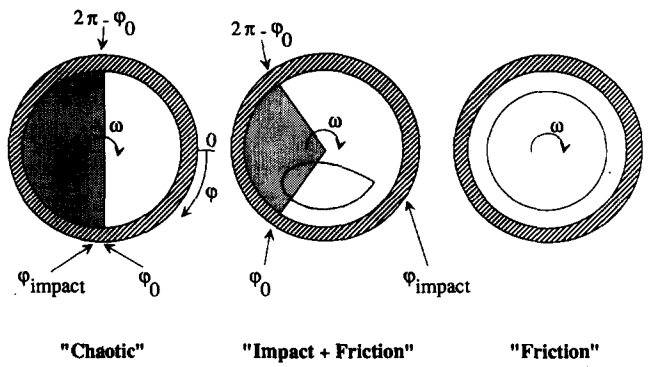

Fig. 2. Schematic representation of the ball trajectory by its centre of mass ($a = 67.5$ mm; $b = 20$ mm). In the "chaotic" mode, the ball impacts the surface in the forbidden domain, and the trajectory cannot be calculated. In the "impact + friction" mode, the ball follows a well-defined trajectory. In the "friction" mode, the ball never leaves the surface of the milling container.

3. Experimental observations

For a qualitative and quantitative evaluation of the modes of a PBM, two different approaches have been considered. In the first the movement of the balls inside a mill is recorded and compared with the calculated movement of the balls. A commercial mill (Retsch, type PM4) was suitable for this purpose. The second approach consists of the analysis of one property of milled powders in order to assess the influence of varying velocity ratio on that property. A versatile mill designed at the Centre National de la Recherche Scientifique (CNRS) [9] was used for this purpose. The

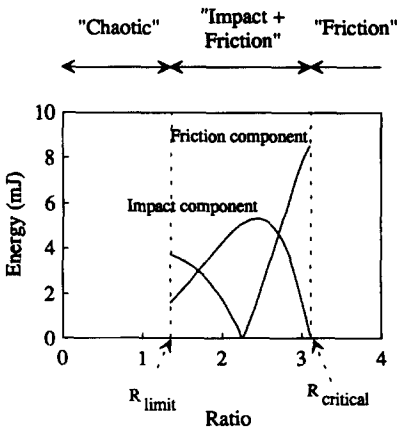

Fig. 3. Calculated impact and friction components of the energy release at time of impact in the "impact + friction" mode as a function of the milling ratio R (ball force, 0.04 N).

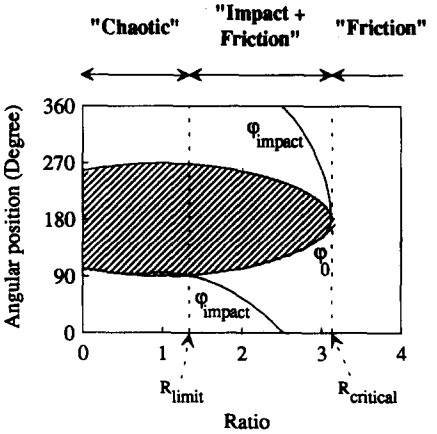

Fig. 4. Schematic representation of the calculated milling modes of a PBM. For one given ratio, the ball moves on a vertical line (see text for explanation). A ball cannot be on the inner milling wall in the shaded domain.

TABLE 1. Parameters of the PBM used in the experiments

	a (mm)	b (mm)	R
CNRS	75	20	Any
Retsch	150	50	2.0

geometrical parameters of the mills used are summarized in Table 1.

The experimental procedures and results of these two series of experiments are presented separately.

3.1. Recorded ball trajectory

3.1.1. Experimental details

In order to allow the observation of the movement of balls in the PBM produced by Retsch, a new fixture was developed which contained a transparent cover. Grinding containers of 500 ml were used with hardened steel balls. The following parameters were varied: size of balls, 6.25 and 10 mm; total mass of balls, from 150 to 1200 g; roughness of the walls and balls, by the use of clean or "dirty" containers and balls which had already been used for other milling experiments; rotation speed Ω of the sun disc, from 50 to 260 rev min^{-1}, as controlled by a tachometer. Two recording film techniques were used. By successive photographic pictures (exposure durations of 1 ms), one obtains an overall view of the position of the balls in the milling container. As a second technique, a high speed Hycam (model 41-0004 from Redlake) camera was operated with exposure durations of 0.25 and 0.5 ms, which allows observation of ball movement in the milling container.

3.1.2. Results

The variation in the parameters yields no fundamental difference concerning the ball trajectories. A typical photograph of the milling vial is presented in Fig. 5(a) and the calculated ball trajectory is provided for comparison (Fig. 5(b)). Qualitatively, the balls occupy the area of the milling container predicted by the model. The angles limiting the domain occupied by the balls have been determined from the photographs; they are, within the limits of accuracy of the measurement, independent of the milling parameters investigated.

The high speed camera revealed more details about the motion of the balls. It is clear that the balls in Fig. 5 move along the mill surface from right to left; whereas after this they either slide inside the mass or make successive small collisions with other balls while they reach the bottom right-hand part of the area occupied by the balls. The direction of the movement of the balls

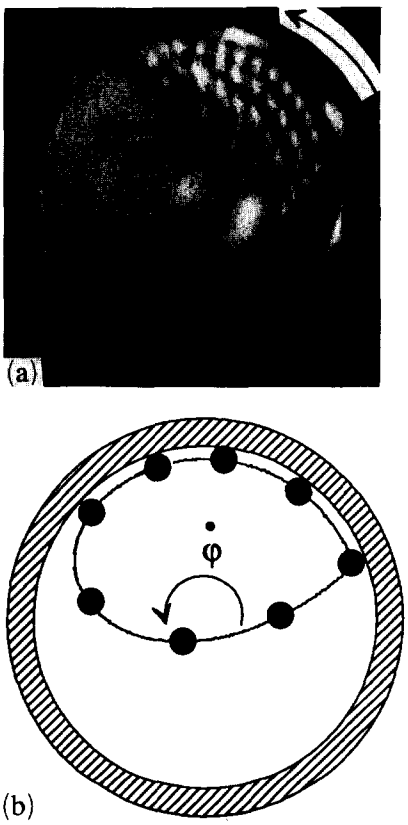

Fig. 5. Comparison of the (a) observed and (b) calculated ball trajectories in a PBM ($a = 150$ mm; $b = 50$ mm; $R = 2.0$; $\Omega = 200$ rev min^{-1}). The arrow indicates the direction of the movement of the balls on the surface.

is in agreement with that calculated. Nevertheless, there is no sign that any ball leaves the surface of the milling container to make a clear single collision after the trajectory in the mill.

3.2. Milling of copper powders

3.2.1. Experimental details

In order to determine experimentally the influence of the ratio R on the milling behaviour, the CNRS mill was used, equipped with vials of 125 ml and 18 balls of 10 mm diameter. Spherical Cu powders were prepared by plasma processing [11], allowing easy observation of the deformation induced by the milling process by scanning electron microscopy (SEM). Powders were about 100–150 μm in diameter. For each experiment, 10 g of powders were sealed in vials filled in Ar. Based on the geometrical parameters of the mill and the model developed, ratios of 1, 2.25 and 4 were selected for the experiments. They correspond to the three milling regimes revealed by the model (see Fig. 2). The rotation speed of the sun disc is 200 rev min^{-1}. Milling durations of up to 7.2 ks were considered. The micro-

hardness of the powders is measured under a load of 0.1 N; each value is the mean of ten measurements.

3.2.2. Results

Figure 6 presents the evolution of the microhardness as a function of the milling duration for R values of 1, 2.25 and 4. Typical morphologies of the powders at milling durations of 1.8 and 7.2 ks are given. Two totally different behaviours have been observed. For $R = 1$, strong interactions are observed as indicated by the faceted morphology of the powders even after very short milling durations. The microhardness increases rapidly with increasing milling time, reaching a plateau value of about 1.3 GPa after 1.8 ks. Further milling results in a reduction in the spreading. For higher ratios ($R = 2.25$ and 4), the microhardness measurements cannot be differentiated. The mean value as well as the spreading are similar. The rate of increase is much smaller than for $R = 1$, and the mean value reached after 7.2 ks is still far from the plateau reached when milling with $R = 1$. It is evident from the SEM images that the interactions are less numerous and less intense when $R = 2.25$ or 4 than when $R = 1$. Two interaction modes can be identified: a low efficiency mode ($R = 2.25$ or 4) and a high efficiency mode ($R = 1$). In the high efficiency mode, not only the frequency but also the energy of the interactions is higher than in the low efficiency mode.

4. Discussion

The results obtained in the modelling and their applicability to the MA process are discussed. The interpretation of the microhardness values of pure metal powders in terms of the deformation modes during milling has been presented in a separate paper [12].

The trajectories of the balls have been calculated with the assumption that a single ball was present in the mill. In practice, several balls are used in a milling experiment. With the hypothesis selected, the addition of other balls does not influence the trajectory calculated as long as the balls do not come into contact with each other. At that time, several layers of balls are formed and balls within different layers will possibly interfere.

The main result of the modelling is the distinction of three modes of operation of a PBM. The discussion is limited to positive values of milling ratios. Similarly to conventional ball mills, a critical speed exists above which a reduced grinding action is expected. The expression of the critical speed obtained here is in agreement with the formula of Lloyd *et al.* [13] when expressed in the same axes system. By analogy with the work of Burgio *et al.* [10], our model also defines a milling mode involving impact and friction. Most commercial mills (such as Fritsch or Retsch) are designed to operate in this mode. The theoretical power P^* transferred to the powders is proportional to the intensity of a single-ball–powder interaction Ω^2 and to the frequency ω of such an event [14]. In our work, we show that there is another operative mode when R is smaller than R_{limit}. It is called the "chaotic mode" and will be discussed later.

Visual observation of ball movement was expected to confirm the theory. While the mill is operated in conditions where impact is predicted to occur, the balls are not observed to fly into the milling chamber (Fig. 5). A systematic analysis of the pictures indicates that there is agreement between modelling and experiments on two points. The first is the angle φ_0 which is approximately equal to the calculated value. The second is the direction of the motion of the balls in the milling container. The poor agreement between the calculated and observed trajectory can primarily be explained by the lack of adherence of the balls on the surface of the milling containers. Even when milling is performed in dirty containers in which slipping of the balls on the surface of the container is reduced, the balls do not follow the calculated trajectory. Interactions are occurring in the mass of the balls and are quite similar to interactions in a conventional horizontal ball mill. Also small collisions between balls of different layers occur.

The ball–powder interactions are similar for a broad range of milling ratios in the PBM corresponding to the domains "impact + friction" or "friction" (Fig. 4), and they do not involve impact. As a conclusion a quantification of the ball–powder interaction by this model is not possible in the "impact + friction" milling mode. The interactions are occurring during sliding or rolling of the balls on the inner wall of the mill.

In our experiments on Cu powders, the same hardness for powders milled at ratios of 2.25 and 4 is explained by the previous discussion; the milling modes are similar for these two R values. Nevertheless, a much more efficient milling has been observed at a milling ratio of 1 and the morphological evolution of the Cu powders indicates a very different interaction mode. This milling ratio corresponds to a chaotic mode, and our model can qualitatively be used for the description of this behaviour.

At low R values, the model predicts a different behaviour; the balls are pushed in a region where they will touch the inner mill wall and then will be directly projected inside the mill. The "chaotic" milling mode can be described well by the predicted angle φ_0 and the direction of the ball motion; the model explains the high efficiency observed at low R values ($R < R_{\text{limit}}$).

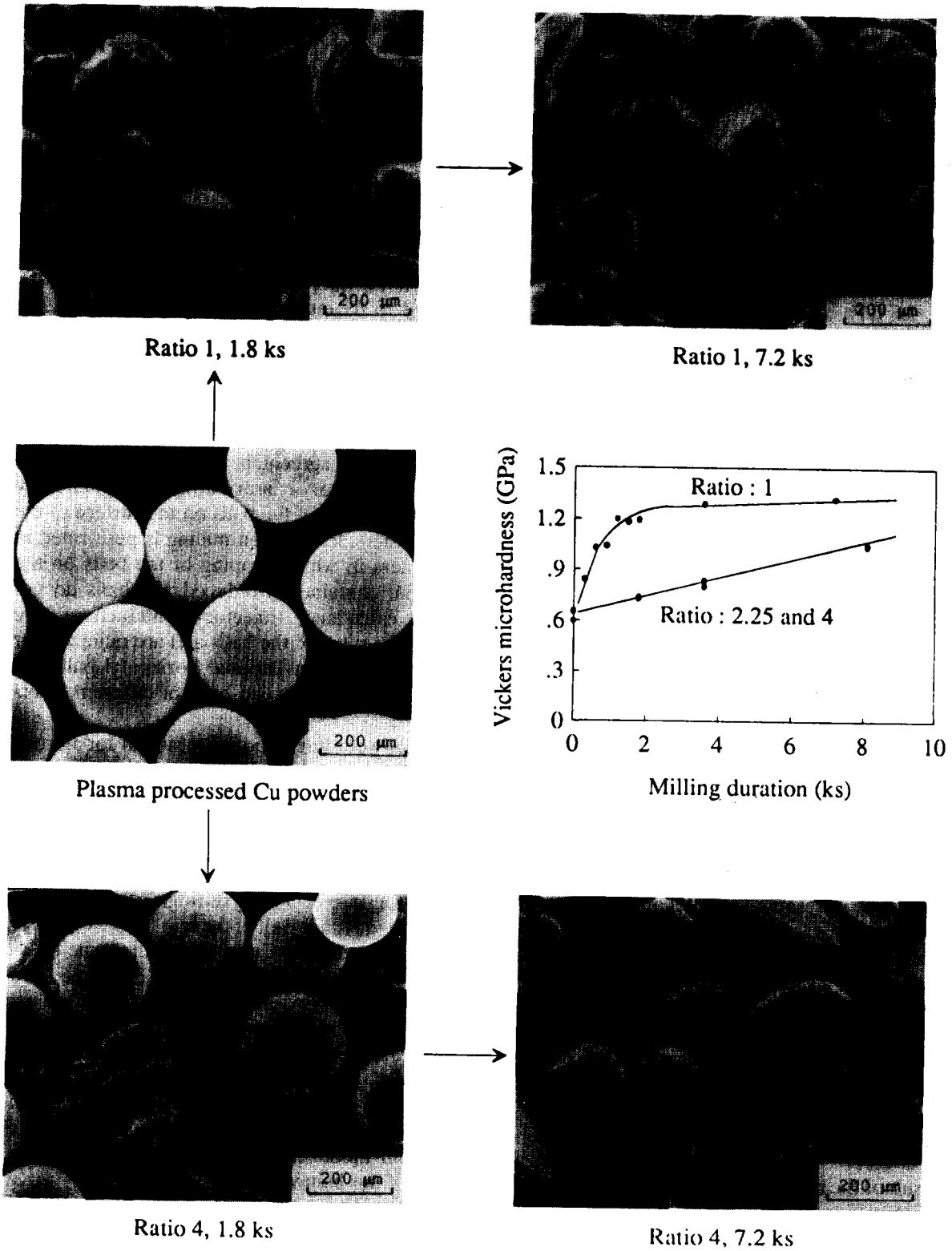

Fig. 6. Hardness and morphological evolution as a function of time for Cu powders milled at ratios corresponding to the "chaotic" mode ($R = 1$), "impact + friction" mode ($R = 2.25$) and "friction" mode ($R = 4$). The morphologies and hardnesses of powders milled at $R = 2.25$ and 4 are similar.

Experiments on the amorphization of intermetallics [9] indeed confirm the concept of efficient milling. Even for a very low ratio ($R=0.1$ at $\Omega=500$ rev min^{-1}), full amorphization was observed. On the contrary, for the same rotation velocity Ω, raising R above 1 reduces the efficiency of milling and only partial amorphization is observed.

All the work presented here is related to typical milling conditions of a commercial PBM, which are also the milling conditions in most published work (see for example refs. 8 and 10). A better agreement between model and experiments could possibly be obtained at very high Ω values. It has indeed been shown with experimental mills that there is a limiting rotational velocity above which full amorphization occurs. For Ni–Zr powders, this value corresponds to a rotation velocity Ω equal to 300 rev min^{-1} [14], which cannot be reached with our mill. Nevertheless, even at higher Ω values, full amorphization would only be expected at low R values, typically less than unity as was observed by Gaffet and Yousfi [15].

5. Conclusions

(1) The comparison of the calculated and experimentally observed trajectories of balls in a PBM reveals that the mode of operation involving impact on the surface following a predicted trajectory has not been observed. Thus it is not possible to calculate values of energies for the ball–powder interaction.

(2) The modelling explains the very efficient milling observed at low ratios of velocities; the milling involves a more chaotic motion of the balls and possibly much stronger interactions.

Acknowledgments

The authors would like to thank E. Gaffet (CNRS) for use of the experimental ball mill. Fruitful discussions with V. Van Kemenade (Louvain-la-Neuve) and E. Gaffet were appreciated.

References

1 R. B. Schwarz and W. L. Johnson, *Phys. Rev. Lett., 51* (1983) 415.
2 M. Oehring and R. Bormann, *Mater. Sci. Eng., A134* (1991) 1330–1333.
3 J. S. Benjamin, *Metall. Trans., 1* (1970) 2943–2951.
4 R. C. Benn, P. K. Mirchandani and A. S. Watwe, in A. H. Clauer and J. J. deBarbadillo (eds.), *Solid State Powder Processing*, Metallurgical Society of AIME, Warrendale, PA, 1990, pp. 157–171.
5 C. C. Koch, *Mater. Sci. Technol., 15* (1991) 193–245.
6 D. R. Maurice and T. H. Courtney, *Metall. Trans. A, 21* (1990) 289–303.
7 P. Le Brun, *Internal Rep.*, 1989 (Katholieke Universiteit Leuven).
8 J. Eckert, L. Schultz and K. Urban, *Z. Metallkd., 81* (12) (1990) 862–868.
9 E. Gaffet, *Mater. Sci. Eng., A132* (1991) 181–193.
10 N. Burgio, A. Iasonna, M. Magini, S. Martelli and F. Padella, *Proc. Int. Conf. on Amorphisation by Solid State Reaction, February 21–23, 1990*, in *J. Phys. (Paris), Colloq. C4, 51* (1990) 265–271.
11 A. Geibel, P. Verstreken, L. Froyen, O. Van Der Biest, L. Delaey, M. Poorteman, P. Barbary and F. Cambier, *Acta Technica Belgica Metall., 4* (1990) 111–119.
12 P. Le Brun, E. Gaffet, L. Froyen and L. Delaey, *Scr. Metall. Mater., 26* (1992) 1743–1748.
13 P. J. D. Lloyd, A. A. Bradley, A. L. Hinde, K. H. Santon and K. Schymura, *Engineering and Mining J.*, (December 1982) 50–54.
14 G. Martin and E. Gaffet, *Proc. Int. Conf. on Amorphisation by Solid State Reaction, February 21–23, 1990*, in *J. Phys. (Paris), Coll. C4, 51* (1990) 71.
15 E. Gaffet and L. Yousfi, *Proc. Int. Symp. on Mechanical Alloying, Kyoto, May 7–10, 1991*, Trans. Tech., Zürich, 1991, Paper 25-6.

Appendix A: Nomenclature

a	distance from the centre of the sun disc to the centre of the milling container
$\boldsymbol{a}_\alpha$	axis system attached to the sun disc
b	radius of the milling container
F	square of the distance between a ball and the surface of the milling container
$\boldsymbol{I}_\alpha$	inertial axis system
$\boldsymbol{p}$	vector of components (p_1, p_2) in the system $\boldsymbol{I}_\alpha$ defining the initial position of a ball at $t=0$
P^*	power input during ball milling
R	ω/Ω, ratio of the milling velocities
R_{critical}	ratio above which the balls constantly stick on the surface of the milling container
R_{limit}	ratio at which the transition between chaotic and impact modes of milling occurs
t	time
$\boldsymbol{v}$	vector of components (v_1, v_2) in the system $\boldsymbol{I}_\alpha$ defining the velocity of a ball at $t=0$
$\boldsymbol{x}$	vector of coordinates (x_1, x_2) expressing the free flight of the ball in the $\boldsymbol{a}_\alpha$ system
$\boldsymbol{y}_\alpha$	axis system for the milling container

Greek letters

α	1 or 2, indices for the axes
θ	angle of rotation of the sun disc towards the inertial system
θ_0	value of θ at $t=0$
φ	angle of rotation of the milling container towards the sun disc

φ_0 value of φ at $t=0$, where $t=0$ is determined by the launching of a ball
ω $d\varphi/dt$, rotation velocity of the milling container
Ω $d\theta/dt$, rotation velocity of the sun disc

Appendix B: Kinetic relations for a planetary ball mill

From Fig. 1 and classical rigid body mechanics, once a ball is free to move, without any constraint or interaction, it will follow a linear motion in the inertial system $\boldsymbol{I}_\alpha$:

$$\boldsymbol{x} = v_1 t \boldsymbol{I}_1 + v_2 t \boldsymbol{I}_2 + p_1 \boldsymbol{I}_1 + p_2 \boldsymbol{I}_2$$

The position (p_1, p_2) of the ball on the surface of the mill at the instant of detachment is obtained from

$$\boldsymbol{p} = a\boldsymbol{a}_1 + b\boldsymbol{y}_1$$

This relation is expressed in the $\boldsymbol{I}_\alpha$ system and calculated at $t=0$, where $\theta=\theta_0$ and $\varphi=\varphi_0$:

$$p_1 = a\cos\theta_0 + b\cos(\theta_0 - \varphi_0)$$

$$p_2 = a\sin\theta_0 + b\sin(\theta_0 - \varphi_0)$$

The components of the velocity vector (v_1, v_2) at the instant of detachment are obtained from $d\boldsymbol{p}/dt$ calculated at $t=0$:

$$v_1 = -a\frac{d\theta}{dt}\sin\theta_0 - b\left(\frac{d\theta}{dt} - \frac{d\varphi}{dt}\right)\sin(\theta_0 - \varphi_0)$$

$$v_2 = a\frac{d\theta}{dt}\cos\theta_0 + b\left(\frac{d\theta}{dt} - \frac{d\varphi}{dt}\right)\cos(\theta_0 - \varphi_0)$$

Appendix C: Determination of the angle φ_0

The function $F = x_1^2 + x_2^2 - b^2$ determines the square of the distance between the ball and the surface. At $t=0$, the ball is on the surface of the mill, and $F=0$. Analytically, it can also be verified that $dF/dt=0$ at $t=0$. At $t=dt$, dF/dt becomes slightly negative or positive. The useful condition for determining whether a ball is stable or not on the surface of the mill is given as follows: $d^2F/dt^2(0)>0$, the ball is pushed against the mill; $d^2F/dt^2(0)<0$, the ball is attracted to the interior of the mill; $d^2F/dt^2(0)=0$, angle φ_0 corresponds to the transition. The solution of the equation

$$\frac{d^2F}{dt^2(0)} = 2(dx_1)^2 + 2x_1(d^2x_1) + 2(dx_2)^2 + 2x_2(d^2x_2) = 0$$

gives eqn. (2):

$$\varphi_0 = \arccos\left(-\frac{b}{a}(1-R)^2\right)$$